the FEBS Journal

Dominant-negative effect of truncated mannose 6-phosphate/insulin-like growth factor II receptor species in cancer

Jodi L. Kreiling[1,*], Michelle A. Montgomery[2,*], Joseph R. Wheeler[2], Jennifer L. Kopanic[2], Christopher M. Connelly[2], Megan E. Zavorka[2], Jenna L. Allison[2] and Richard G. MacDonald[2]

1 Department of Chemistry, University of Nebraska at Omaha, Omaha, NE, USA
2 Department of Biochemistry and Molecular Biology, University of Nebraska Medical Center, Omaha, NE, USA

Keywords
dimerization; dominant negative; ectodomain shedding; mannose 6-phosphate receptor; truncation mutants

Correspondence
R. G. MacDonald, Department of Biochemistry and Molecular Biology, University of Nebraska Medical Center, 985870 Nebraska Medical Center, Omaha, NE 68198-5870, USA
Fax: +1 402 559 6650
Tel: +1 402 559 7824
E-mail: rgmacdon@unmc.edu

*These authors contributed equally to this work

(Received 22 November 2011, revised 2 May 2012, accepted 4 June 2012)

doi:10.1111/j.1742-4658.2012.08652.x

Oligomerization of the mannose 6-phosphate/insulin-like growth factor II receptor (M6P/IGF2R) is important for optimal ligand binding and internalization. *M6P/IGF2R* is a tumor suppressor gene that exhibits loss of heterozygosity and is mutated in several cancers. We tested the potential dominant-negative effects of two cancer-associated mutations that truncate M6P/IGF2R in ectodomain repeats 9 and 14. Our hypothesis was that co-expression of the truncated receptors with the wild-type/endogenous full-length M6P/IGF2R would interfere with M6P/IGF2R function by heterodimer interference. Immunoprecipitation confirmed formation of heterodimeric complexes between full-length M6P/IGF2Rs and the truncated receptors, termed Rep9F and Rep14F. Remarkably, increasing expression of either Rep9F or Rep14F provoked decreased levels of full-length M6P/IGF2Rs in both cell lysates and plasma membranes, indicating a dominant-negative effect on receptor availability. Loss of full-length M6P/IGF2R was not due to increased proteasomal or lysosomal degradation, but instead arose from increased proteolytic cleavage of cell-surface M6P/IGF2Rs, resulting in ectodomain release, by a mechanism that was inhibited by metal ion chelators. These data suggest that M6P/IGF2R truncation mutants may contribute to the cancer phenotype by decreasing the availability of full-length M6P/IGF2Rs to perform tumor-suppressive functions such as binding/internalization of receptor ligands such as insulin-like growth factor II.

Structured digital abstract

- **Rep9F** physically interacts with **WT-M** by anti tag coimmunoprecipitation (View Interaction: 1, 2)
- **Rep14F** physically interacts with **WT-M** by anti tag coimmunoprecipitation (View Interaction: 3, 4)

Abbreviations

1–15F, truncation construct containing the entire ectodomain region; ADAM, a disintegrin and metalloproteinase; BSA, bovine serum albumin; CCM, concentrated conditioned medium; CREG, cellular repressor of E1A-stimulated genes; HBS, HEPES-buffered saline; HEK, human embryonic kidney; HEPES, 4-(2-hydroxyethyl)-1-piperazineethanesulfonic acid; HMM, high molecular mass; IGF, insulin-like growth factor; M6P, mannose 6-phosphate; M6P/IGF2R, mannose 6-phosphate/insulin-like growth factor II receptor; MMP, matrix metalloproteinase; OPA, 1,10-orthophenanthroline; PMP, pentamannosyl 6-phosphate; Rep9F and Rep14F, truncated receptors; WT-M, Myc-tagged wild-type M6P/IGF2R.

Introduction

The mannose 6-phosphate/insulin-like growth factor II receptor (M6P/IGF2R) is a multifunctional transmembrane receptor of the p-lectin family that serves as both a tumor suppressor and in lysosome biogenesis [1,2]. This 300 kDa glycoprotein has four major structural domains: the N-terminal signal sequence, a short C-terminal cytoplasmic region, a single transmembrane domain, and a large extra-cytoplasmic region or ectodomain. The ectodomain comprises 15 homologous repeating segments (termed mannose 6-phosphate receptor homology domains), each $\sim$ 147 amino acid residues long and sharing 14–28% sequence identity [1,3]. The M6P/IGF2R binds two major classes of ligand, M6P-bearing and non-M6P polypeptides, most of which bind to the receptor's ectodomain [3,4]. Three M6P-binding sites have been mapped to critical residues within repeats 3 and 9 (high-affinity) and repeat 5 (low-affinity) of the ectodomain [3]. Although these binding sites share the overall canonical fold of the mannose 6-phosphate receptor homology domains, each has distinctive binding properties, manifested in differences in pH optima, preferences for binding M6P mono- versus di-ester structures, and inter-repeat interactions required to form a functional binding site [2].

The M6P-bearing ligands include lysosomal acid hydrolases, transforming growth factor β, proliferin, thyroglobulin and granzyme B [2]. The non-M6P ligands of the M6P/IGF2R include the mitogen, insulin-like growth factor II (IGF-II) retinoic acid and plasminogen. The binding site for IGF-II has been mapped to repeat 11 of the ectodomain, with structural stabilization of the binding region contributed by the 13th repeat [3]. Structural studies have shown that IGF-II binds within a hydrophobic pocket at the end of a β-barrel structure [5]. Binding of IGF-II plays an important role in the regulation of IGF-II action in target cells, leading to uptake into the cell and eventual degradation of IGF-II within lysosomes. This decrease in IGF-II availability reduces the interaction of IGF-II with insulin-like growth factor I receptors, contributing to the anti-proliferative and tumor-suppressive effects of the M6P/IGF2R [6–8]. Plasminogen binds to a site mapped to ectodomain repeat 1; this function of the M6P/IGF2R is thought to play a role in mediating proteolytic activation of plasminogen to plasmin [9].

Several groups have provided crystal structure data for portions of the M6P/IGF2R ectodomain, allowing insight into and model predictions of the overall structure of this large receptor [5,10–12]. Structures of repeat 11, repeats 1–3, repeats 11–13 and repeats 11–14 have been determined. The high level of sequence identity between the ectodomain repeats (14–28%) and/or between the repeats and the ectodomain of the cation-dependent M6P receptor (16–38%) account for structural similarities among the repeats, including conserved disulfide bond organization, and the overall flattened β-barrel structure of the repeats. The current model proposes that the M6P/IGF2R ectodomain is composed of tri-repeat units (repeats 1–3, 4–6 and 7–9) that stack on each other with a superhelical twist, with the distal six repeats of the ectodomain forming a larger hexameric unit (repeats 10–15) [5]. In this model, repeats 1–3 together form a high-affinity M6P binding site, repeats 4–6 include a low-affinity M6P binding site, repeats 7–9 encompass a second high-affinity M6P binding site, and repeats 10–15 include the high-affinity IGF-II binding site and the region thought to stabilize dimer formation (repeat 12) [5,13].

The M6P/IGF2R was long thought to function as a monomer; over the past decade, evidence has accumulated indicating that this receptor actually functions optimally as an oligomer in terms of high-affinity M6P ligand binding and internalization of ligands. York *et al.* [14] showed that binding of phosphomannosylated ligands with multiple M6P moieties, including β-glucuronidase, induced cell-surface oligomerization of the M6P/IGF2R, resulting in more efficient uptake of receptor ligands by cross-bridging M6P/IGF2R molecules. IGF-II binding did not produce the same increase in receptor internalization, consistent with subsequent reports that IGF-II binds independently to both protomers of a dimeric receptor [15]. Byrd *et al.* [16,17] further showed that dimer formation occurred regardless of the state of ligand binding for the receptor, probably mediated by interactions between repeats across receptor molecules. Mapping studies by Kreiling *et al.* [13] showed that inter-subunit interactions appear to occur all along the M6P/IGF2R ectodomain, with particular stability of the dimer conferred by the presence of repeat 12. These findings are supported by the composite model of the receptor assembled by Brown *et al.* [5].

Several studies have reported mutations in the *M6P/IGF2R* gene in various cancers that result in positioning of a nonsense codon in the reading frame with prediction of premature termination, i.e. synthesis of receptors truncated within repeat 9 or repeat 14 of the ectodomain [15,18,19]. To date, there have been no functional studies of these truncated forms of the M6P/IGF2R; in particular, the possibility that they

may form heterodimers with wild-type receptors and act in a dominant-negative manner has not been explored. In order to address how these mutations affect the function of wild-type receptors present in the same cells, we prepared mini-receptors that mimic these cancer-associated mutant receptor forms, termed Rep9F and Rep14F. Our hypothesis was that interaction of the full-length receptor with a truncated receptor in a heterodimeric structure would lead to interference with receptor functions, e.g. impaired IGF-II degradation and lysosomal enzyme sorting. Upon expression of these mutant constructs in HEK 293 cells, truncated receptors were found both within the cells and secreted into the medium. The truncated receptors associated as dimers or in multimeric complexes with full-length endogenous M6P/IGF2R in cells. During experiments to test the possibility of dominant-negative effects on wild-type receptors, we observed marked loss of endogenous receptors from cells as a result of expression of the truncated forms of the receptor. Here we provide evidence that the mechanism for this loss of M6P/IGF2R from cells expressing both the full-length receptor and a truncated form of the receptor is ectodomain shedding. We conclude that truncation mutants of *M6P/IGF2R* that occur in cancer cells may interfere with function of the normal gene product by dimerization, leading to cleavage and an enhanced rate of shedding of the imbalanced heterodimeric complex.

Results

Transient expression of wild-type M6P/IGF2R with truncated receptors leads to destabilization of wild-type receptor expression

Several cancer-associated mutations of the *M6P/IGF2R* gene are predicted to synthesize truncated forms of the receptor. In one such case, mutations arise from microsatellite instability of a poly(G) tract from nucleotides 4089–4096; one- and two-base insertions in this tract were observed in gastrointestinal cancers [18] and squamous cell carcinoma of the lung [20]. The resultant frameshift places an in-frame nonsense codon downstream of this site and causes premature termination of the protein. The deleted region encompasses part of repeat 9, all of repeats 10–15, the transmembrane region and the cytoplasmic domain, so there is potential for interference with both M6P and IGF-II binding functions. In another case, a C:G to A:T transversion observed in hepatocellular carcinoma at *M6P/IGF2R* nucleotide 6410 created an alternative splice site within intron 40 [15]. Abnormal splicing brings a nonsense codon in-frame immediately after Ser2023, producing a receptor truncated within repeat 14 that lacks repeat 15 and the transmembrane and cytoplasmic domains.

In order to study the effects of expression of truncated forms of M6P/IGF2R on the oligomeric structure and function of the wild-type receptor, two truncation mutations bearing C-terminal FLAG tags, termed Rep9F and Rep14F, were designed and synthesized to mimic these naturally occurring receptor mutants (Fig. 1). In addition to the cancer-associated truncated constructs, a truncation construct containing the entire ectodomain region (1–15F) was evaluated in conjunction with a full-length, wild-type receptor construct containing a C-terminal Myc epitope tag (WT-M). Ligand blotting experiments with lysates from cells transfected with each of the truncated receptor constructs were performed to test for ligand-binding properties (Fig. 1D). As predicted by its structure, Rep9F, which contains only one intact binding site for M6P-based ligands, was not able to bind IGF-II, but did bind the M6P pseudoglycoprotein ligand pentamannosyl 6-phosphate–bovine serum albumin (PMP–BSA). All the other constructs (Rep14F, 1–15F, WT-M and endogenous M6P/IGF2R) were able to bind both IGF-II and PMP–BSA (Fig. 1D), indicating that the truncated receptor proteins folded well enough to attain ligand-binding function.

To test whether truncated receptor proteins were expressed at detectable levels in cells, the Rep9F and Rep14F cDNA constructs were transiently expressed by co-transfection with WT-M cDNA into HEK 293 cells. Each truncated construct (Rep9F, Rep14F or 1–15F) was transfected under a total of eight conditions, during which the amount of cDNA for the truncated construct was increased and the amount of WT-M cDNA was held constant. The empty plasmid, pCMV5, was used as a negative control for expression of the tagged proteins (Fig. 2A–E, lane 1). Whole-cell lysates were analyzed for relative expression levels of the receptors by immunoblotting with α-FLAG or α-Myc IgGs (Fig. 2A–C).

Immunoblot analysis revealed that all of the truncated receptors were readily detectable in the HEK 293 cells. However, in each series of transfections, expression of WT-M decreased as a function of increasing input of 1–15F, Rep9F or Rep14F cDNA, even though the input of WT-M cDNA was held constant at 5 μg in each condition tested (Fig. 2A–C, lanes 2–7), suggesting that co-expression of M6P/IGF2R constructs lacking the transmembrane and cytoplasmic domains somehow inhibited expression of WT-M. Quantitative analysis of these data indicated that the

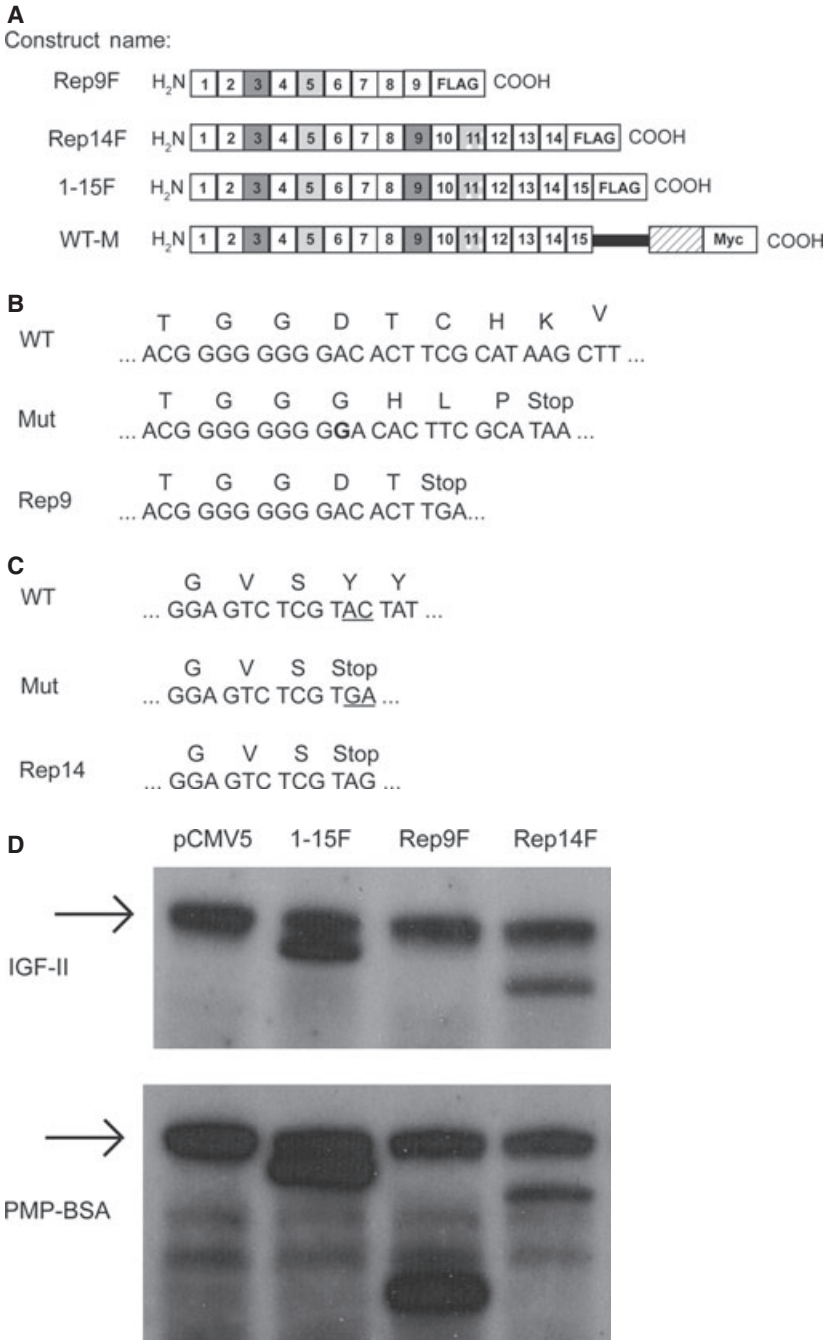

Fig. 1. M6P/IGF2R constructs and cancer-associated truncation mutations. (A) Receptor constructs. Squares represent the repeating units (mannose 6-phosphate receptor homology domains) of the M6P/IGF2R ectodomain. The dark gray boxes represent the locations of high-affinity M6P binding sites (repeats 3 and 9). The light gray boxes represent the low-affinity M6P binding site in repeat 5, and the stippled gray boxes indicate the location of the principal IGF-II binding site in repeat 11. Rectangles indicate addition of the FLAG or Myc epitope tags to the C-termini of the proteins. The solid black bar represents the transmembrane domain of the full-length M6P/IGF2R, and the hatched rectangle indicates the M6P/IGF2R cytoplasmic region. (B,C) Oligonucleotides were created to amplify the indicated regions of the human M6P/IGF2R cDNA sequence, thereby creating termination codons that mimic the truncations resulting from naturally occurring mutants (Mut). (B) Insertion of a G (bold) within the poly(G) tract causes a frameshift in the mutant, resulting in an early termination codon. (C) A C:G to A:T transversion downstream of the region shown, located in *M6P/IGF2R* exon 40, creates a novel splice site that leads to premature termination after Ser2023. (D) Ligand blots of lysates (50 μg protein per lane) from cells transfected with cDNAs encoding the various truncated M6P/IGF2R species. Blots were probed with ^{125}I-IGF-II or ^{125}I-PMP–BSA. The arrow indicates ligand binding to the endogenous M6P/IGF2R.

effects of the Rep9F truncated receptor resulted in ~ 40–50% WT-M protein being detected at the highest ratio of WT-M to Rep9F (4 : 1 Rep9F:WT-M) (Fig. 2C, lane 7). In contrast, Rep14F potently suppressed recovery of the WT-M protein to levels < 10% of control at the highest transfection ratio (4 : 1 Rep14F/WT-M) (Fig. 2B, lane 7). Expression of the 1–15F truncated receptor also suppressed recovery of the WT-M protein (Fig. 2A, lane 7). These results indicate the possibility that formation of oligomeric complexes between full-length and truncated M6P/IGF2Rs destabilizes expression of the full-length receptor in HEK 293 cells.

To test whether this same phenomenon also affected the endogenous M6P/IGF2R, this experiment was repeated by transfecting HEK 293 cells with increasing concentrations of the truncated Rep9F and Rep14F constructs (Fig. 2D,E). The amount of endogenous

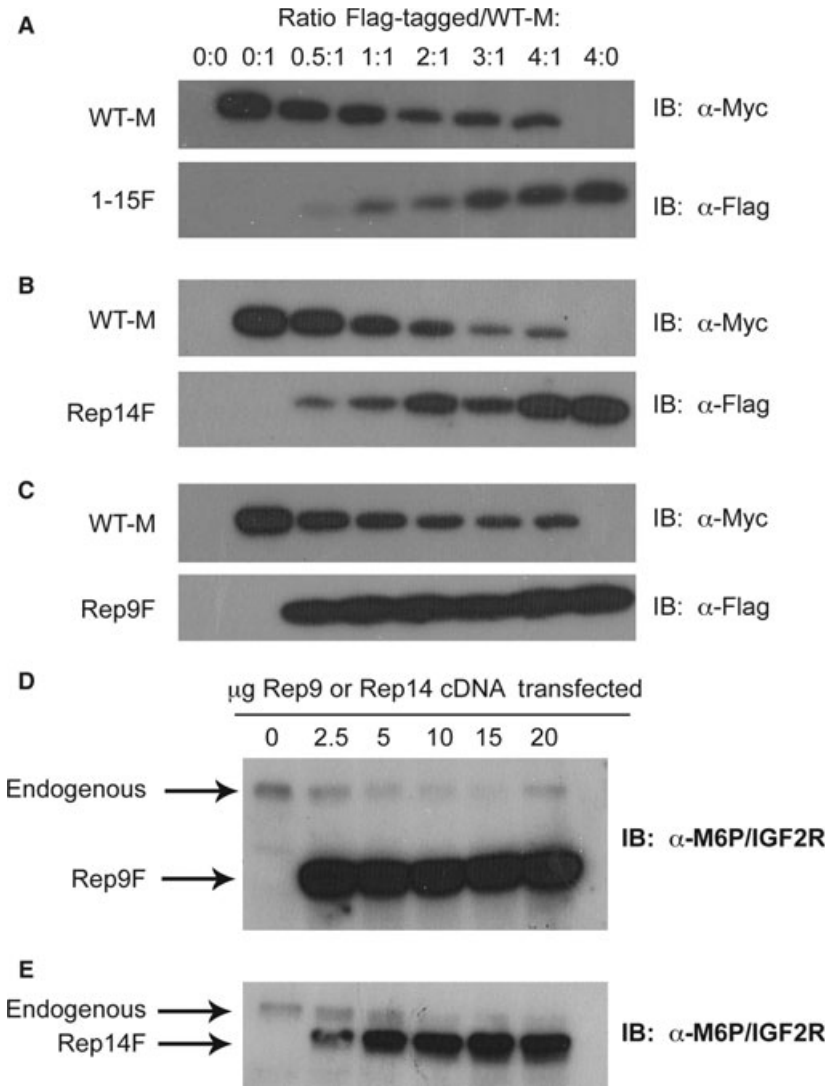

Fig. 2. Transient expression of M6P/IGF2R constructs in HEK 293 cells. HEK 293 cells were transfected or co-transfected with the indicated ratios of FLAG-tagged truncated M6P/IGF2R versus WT-M cDNA constructs. The amount of total DNA transfected was adjusted to 25 μg per 100 mm dish by balancing with vector DNA. Aliquots (25 μL) of detergent extracts were resolved by 6% SDS/PAGE, immunoblotted with α-FLAG, α-Myc or α-M6P/IGF2R IgGs, and assayed by autoradiography. A blot representative of at least three transfections is shown: (A–C) co-transfection of WT-M with 1–15F (A), Rep14F (B) or Rep9F (C), or (D,E) single transfection of the indicated amounts of Rep9F (D) or Rep14F (E). Arrows in (D) and (E) indicate expression of the indicated constructs. Regression analysis indicated that the effects of truncated receptors on expression of the full-length receptors were significant: (A) $P < 0.0001$; (B) $P < 0.003$; (C) $P < 0.0002$; (D) $P < 0.015$; (E) $P < 0.004$.

M6P/IGF2R detected in the cell extracts decreased with increasing expression of Rep9F or Rep14F (Fig. 2D,E). These data suggest that transfection of these truncated M6P/IGF2Rs suppresses expression of the exogenous full-length WT-M protein, as well as decreasing levels of the endogenous M6P/IGF2R within cells.

Truncated forms of the M6P/IGF2R dimerize with the full-length M6P/IGF2R

The suppressive effect of the truncated receptors on the full-length M6P/IGF2R may be mediated at the pre- or post-transcriptional levels. The latter possibility implies that co-transfected truncated forms of the M6P/IGF2R interact by dimerization with the full-length receptor. To test this hypothesis, HEK 293 cell lysates containing co-expressed FLAG- and Myc epitope-tagged receptors were analyzed by an immunoprecipitation assay using α-FLAG affinity resin (Figs 3 and 4). Analysis of the immunoblots revealed that essentially all of the expressed FLAG-tagged truncated receptors precipitated with the α-FLAG affinity resin (Figs 3 and 4: compare resin FLAG blot with lysate FLAG blot). The data in Figs 3 and 4 indicate that the Myc-tagged full-length receptor did not immunoprecipitate in the absence of the FLAG-tagged truncated partner (Figs 3 and 4, lane 2), but was detectable in the presence of FLAG-tagged truncated partners (Figs 3 and 4, lanes 3–7). These data indicate that these differentially epitope-tagged M6P/IGF2Rs were capable of association as asymmetric oligomers.

In these experiments, co-transfection of either Rep9F (Fig. 3) or Rep14F (Fig. 4) at increasing ratios of truncated construct to full-length WT-M again suppressed the overall expression of the WT-M protein, as

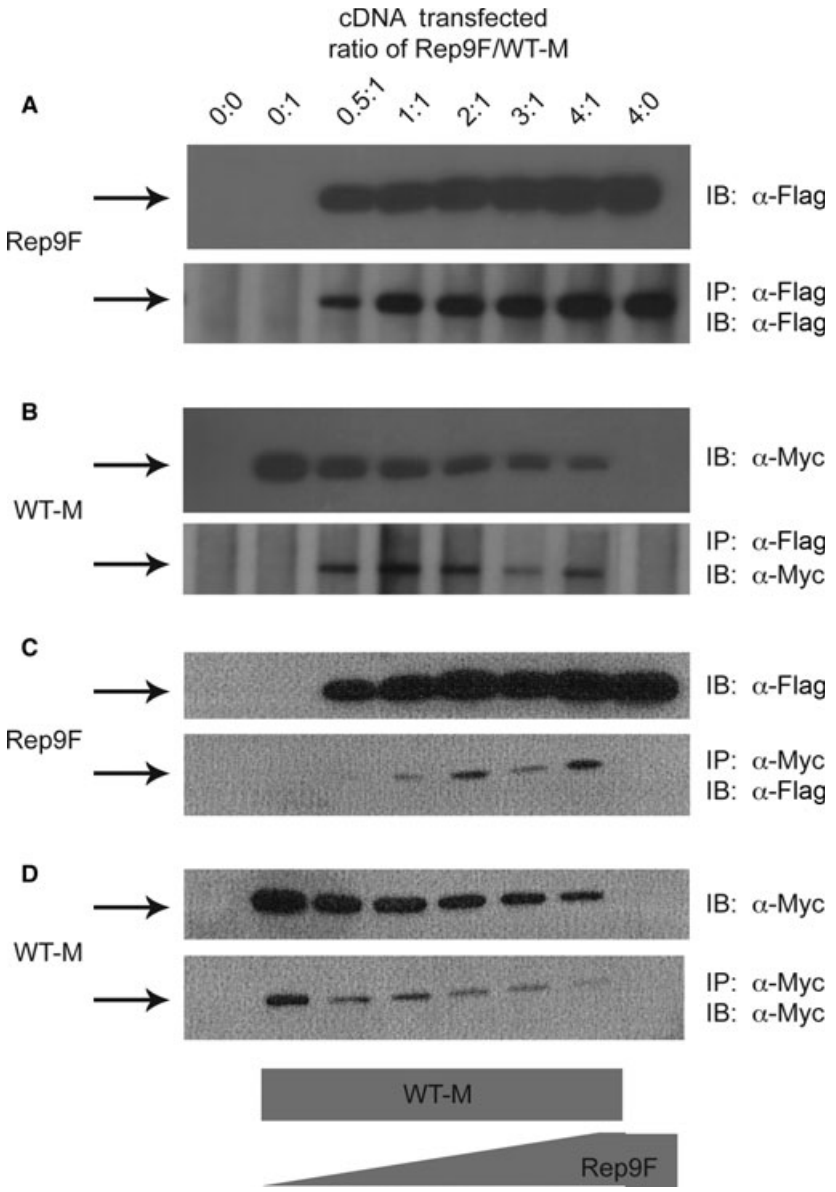

Fig. 3. Co-immunoprecipitation of Rep9F and WT-M receptors from co-transfected HEK 293 cells. The ability of WT-M to co-immunoprecipitate with Rep9F was measured by immunoprecipitation assays. (A,B) Immunoprecipitation with α-FLAG affinity resin. Equal protein amounts (100 μg) of Triton X-100 extracts from HEK 293 cells co-transfected with increasing amounts of Rep9F (0–20 μg) and a constant amount of WT-M (5 μg) cDNA were immunoprecipitated with 8 μL α-FLAG resin in a volume of 0.2 mL. The resin-bound proteins from the resin pellets (lower panels) and samples of lysates that were not immunoprecipitated (upper panels) were resolved by 6% SDS/PAGE, subjected to immunoblot analysis with α-FLAG (A) or α-Myc (B), and assayed by autoradiography. Representative blots are shown. (C,D) α-Myc immunoprecipitation and subsequent immunoblot analysis of Rep9F and WT-M. Equal volumes (20 μL) of detergent extracts from co-transfected HEK 293 cells were incubated with 1 ml α-Myc IgG in a volume of 0.1 ml. Subsequently, aliquots (25 μL) of washed/blocked protein G–Sepharose were added to the reactions to a total volume of 0.2 mL, and incubated further for immunoprecipitation. The pellets were processed and analyzed as in (A) and (B), respectively. The blots shown are representative of three replicate experiments.

indicated by the progressive loss of detectable WT-M with expression of increasing amounts of truncated receptor. This loss of WT-M protein expression was much more pronounced when co-expressed with the Rep14F truncated receptor, such that it was difficult to observe WT-M in co-immunoprecipitation experiments in which the precipitating antibody was anti-FLAG (Fig. 4B). These data indicate that these truncated M6P/IGF2R forms may indeed have dominant-negative effects on M6P/IGF2R availability when expressed in the heterozygous condition in cancer cells.

To ascertain that the observed interactions were not merely a result of use of the α-FLAG affinity resin, reciprocal immunoprecipitation experiments were also performed using α-Myc IgG followed by precipitation with protein G–Sepharose. The data in Figs 3D and 4D indicate that WT-M was immunoadsorbed to the α-Myc matrix as expected. More importantly, when WT-M was used as the bait in co-immunoprecipitation assays, we observed that Rep9F (Fig. 3C, lower panel) and Rep14F (Fig. 4C, lower panel) were readily interacted with WT-M.

One condition that must be fulfilled by the truncated receptors in order to affect M6P/IGF2R functions is that the dominant-negative effect on the full-length M6P/IGF2R seen at the whole-cell level must be reflected in reduced receptor numbers at the cell surface. Thus, to provide a more direct test of this

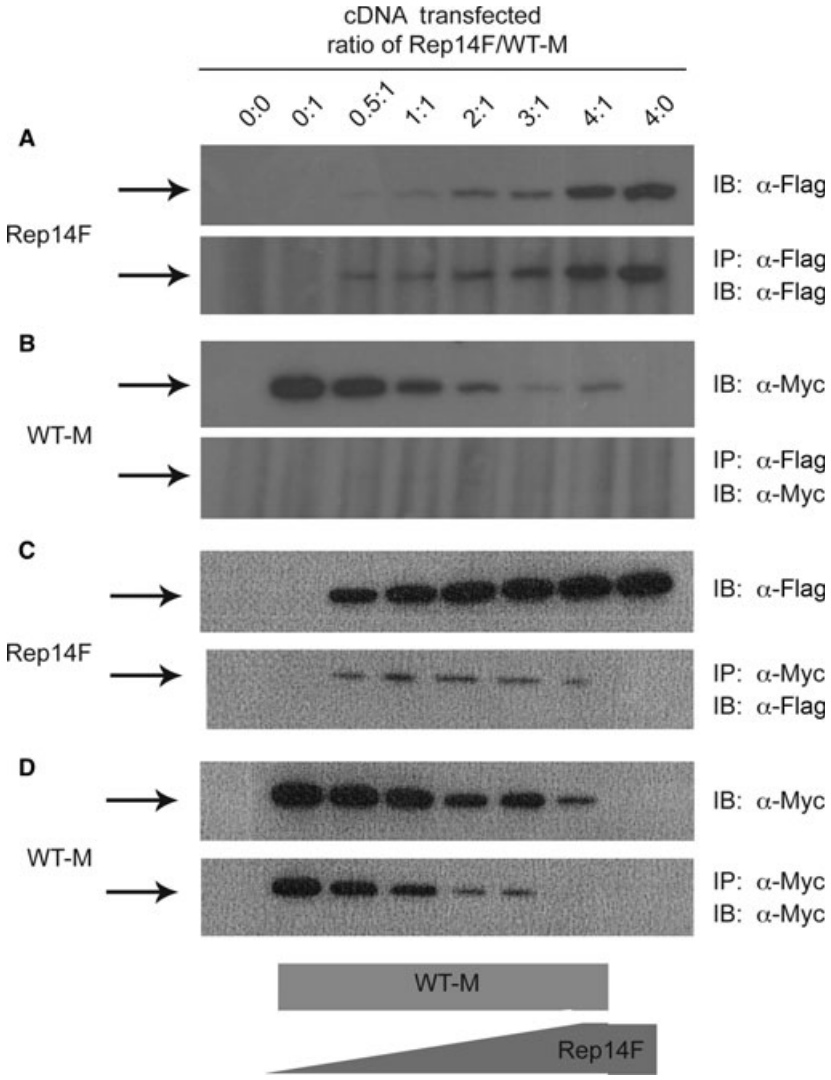

Fig. 4. Co-immunoprecipitation of Rep14F and WT-M receptors from co-transfected HEK 293 cells. The ability of WT-M to co-immunoprecipitate with Rep14F was measured by immunoprecipitation assays as in Fig. 3. (A,B) Immunoprecipitation with α-FLAG affinity resin followed by blotting with α-FLAG (A) or α-Myc (B) IgGs. (C,D) α-Myc immunoprecipitation and subsequent immunoblot analysis of Rep14F and WT-M. The blots shown are representative of three replicate experiments.

hypothesis, we measured the effect of expressing the truncated forms of the receptor on the amount of full-length M6P/IGF2R in plasma membranes of HEK 293 cells (Fig. 5). In this experiment, expression of Rep14F was not as high as seen in some of the earlier experiments; the Rep14F protein is readily detected in the anti-M6P/IGF2R blots, but not so well in the anti-FLAG blots. Nevertheless, expression of either truncated receptor decreased the amount of full-length receptors in lysates, either endogenous M6P/IGF2R or co-transfected WT-M protein (Fig. 5A). Importantly, the same effect was observed in plasma membranes prepared from cells in this same transfection experiment (Fig. 5B). Analysis of the band intensities on anti-M6P/IGF2R blots from three experiments revealed that both Rep9F and Rep14F suppressed the level of full-length endogenous and WT-M receptors in cell lysates by 21–28%. In the plasma membranes, Rep9F was less potent than Rep14F in this regard, producing reductions of 13% and 30%, respectively. Only the effect of Rep14F on the amount of full-length receptor (endogenous M6P/IGF2R or WT-M) was significant in both lysates and plasma membranes. Nevertheless, these data support the conclusion that the effect seen in whole-cell lysates is reflected in plasma membranes, i.e. the cell-surface receptor complement.

Presence of Rep9F or Rep14F does not alter the half-life of the wild-type M6P/IGF2R

To determine whether the apparent loss in expression of the full-length receptor induced by expression of the truncated M6P/IGF2Rs was due to an alteration in the receptor's degradation rate, we examined

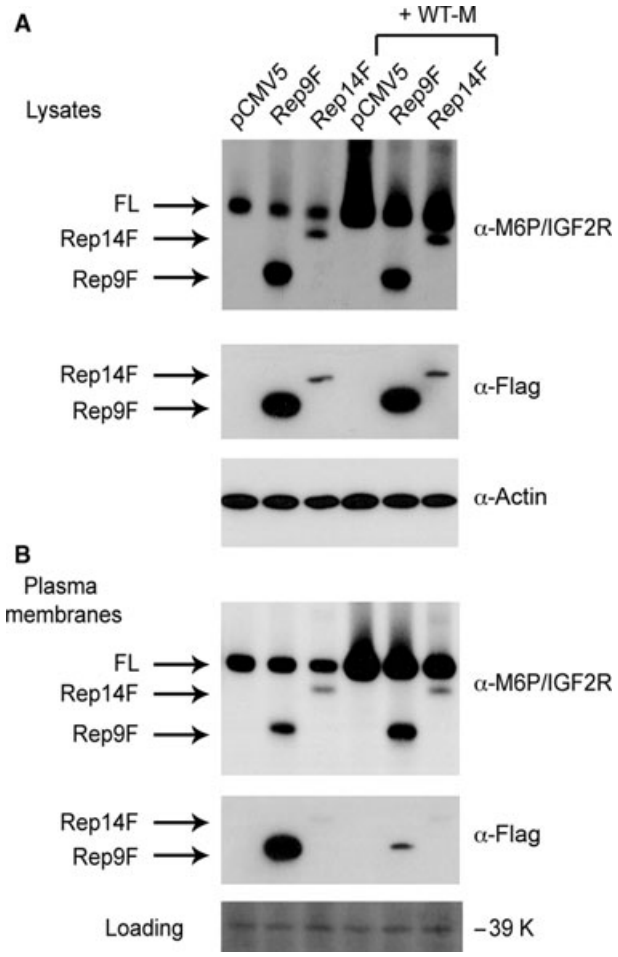

Fig. 5. Effect of truncated receptor expression on the amount of full-length M6P/IGF2R in whole-cell lysates versus plasma membranes. HEK 293 cells were transfected with pCMV5 vector or cDNAs (10 μg) encoding Rep9F or Rep14 alone or by co-transfection with empty vector or 10 μg of cDNA encoding the full-length WT-M receptor, as indicated. The total amount of transfected DNA was 20 μg per dish in all cases. Aliquots (50 μg protein) of detergent extracts (lysates) (A) and plasma membranes (B) were analyzed by immunoblotting with the antibodies indicated on the right. Arrows indicate the various forms of the receptor. The bottom panel in (B) shows a portion of the plasma membrane blot stained with a solution of 0.1% Ponceau S in HBS; the intensity of a 39 kDa band serves as a loading control. One-way ANOVA of the data from three replicate experiments indicated that differences in intensity of the full-length bands were not significant when comparing Rep9F-transfected cells versus pCMV5 vector-transfected cells or cells co-transfected with Rep9F and WT-M. The effect of Rep14F on the intensity of the endogenous receptor bands and the WT-M exogenous receptor bands was significant ($P < 0.025$) in both lysates and plasma membranes.

protein half-lives by metabolic labeling. Metabolic labeling experiments were performed in HEK 293 cells transiently expressing WT-M alone or WT-M in combination with Rep9F or Rep14F. No significant overall differences were observed for the half-lives of WT-M in the presence or absence of Rep9F or Rep14F (data not shown). The half-life calculated for all receptor species was ~ 16 h, which agrees with published values [21,22]. These experiments were also performed with varied chase times, from 6 to 12 h, and in the presence of cycloheximide to inhibit radiolabel re-utilization via protein synthesis during the chase period (data not shown). These experiments resulted in the same calculated half-life of 16 h, and no observed differences among the different receptor species.

Dimer interference effects of the Rep9F and Rep14F truncated M6P/IGF2Rs are not due to receptor degradation by the lysosomal or proteasomal pathways

In order to further investigate the mechanism of loss of WT-M expression when there is an increase in expression of truncated M6P/IGF2Rs, we determined whether the presence of the truncated receptor in complex with full-length receptors triggered some form of targeted degradation of the asymmetric heterodimeric complexes by either the proteasomal or lysosomal degradative pathways.

The involvement of lysosomes in the decreased protein expression of wild-type M6P/IGF2R was first examined by exposing HEK 293 cells that had been transfected with the various truncated and full-length M6P/IGF2R constructs to either 0, 100 or 200 μM chloroquine for 16 h (Fig. 6). Chloroquine is a lysosomotropic agent that accumulates in the lysosomes, causing alkalinization of the lysosomal lumen and thereby inhibiting the activity of acid hydrolases within the organelle [23]. After treatment with chloroquine, expression of each receptor construct was analyzed by immunoblotting with α-FLAG or α-Myc IgGs (Fig. 6). Chloroquine-induced inhibition of lysosomal degradative processes had no apparent effect of the amounts of truncated or full-length receptors recovered in cell lysates, indicating that the wild-type M6P/IGF2R was not trapped in the lysosome by the presence of the truncated receptors (Fig. 6A,B, compare the amount of WT-M protein expressed in the presence of 0–200 μM chloroquine for conditions 3 and 4). As a positive control for lysosomal degradation, the levels of cathepsin D were assessed. As expected, treatment with chloroquine increased the amount of immunodetectable cathepsin D in HEK 293 cell lysates during this same time period (Fig. 6C).

The effect of the 26S proteasomal inhibitor lactacystin [24] was next examined. Cells expressing WT-M,

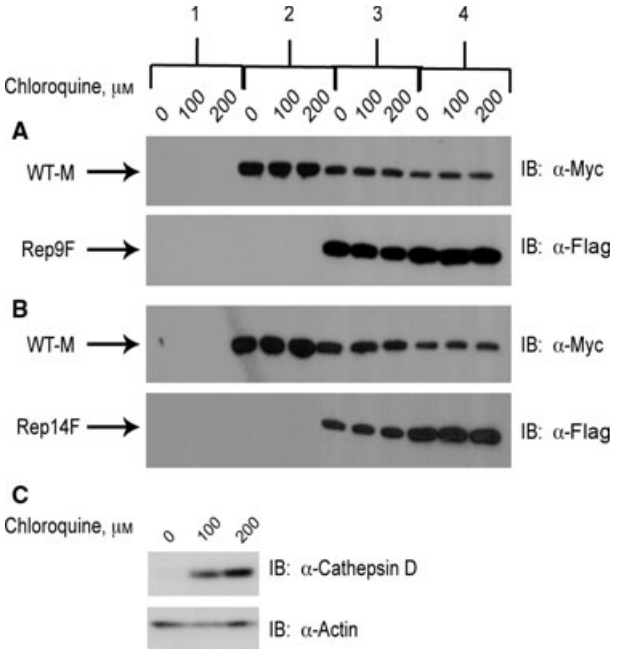

Fig. 6. Lack of effect of chloroquine on degradation of wild-type M6P/IGF2R in response to co-expression with truncated constructs. HEK 293 cells were transfected with the cDNA constructs as indicated: (1) 25 μg pCMV5 vector control; (2) 5 μg WT-M cDNA; (3) 5 μg WT-M + 5 μg mini-receptor cDNAs; (4) 5 μg WT-M + 15 μg mini-receptor cDNAs. Vector control DNA was also added to samples 2 and 3 such that the total amount of DNA transfected per dish was 25 μg. Twenty-four hours after transfection, the cells were treated with the indicated concentrations of chloroquine for 16 h to inhibit lysosome-based protein degradation. Detergent extracts were prepared, and 100 μg of total protein from each lysate condition was resolved by 6% SDS/PAGE, immunoblotted with α-FLAG or α-Myc IgGs, and assayed by autoradiography. Arrows indicate the various forms of the M6P/IGF2R expressed in HEK 293 cells. Blots shown are representative of three transfections: co-transfection of WT-M and Rep9F (A) and WT-M and Rep14F (B). (C) Positive control showing the effect of chloroquine on expression of cathepsin D (α-cathepsin D IgG at 1 : 500 dilution). Within each transfection group, there was no significant effect of chloroquine on the intensities of the WT-M bands: $P > 0.05$ for all comparisons (A,B).

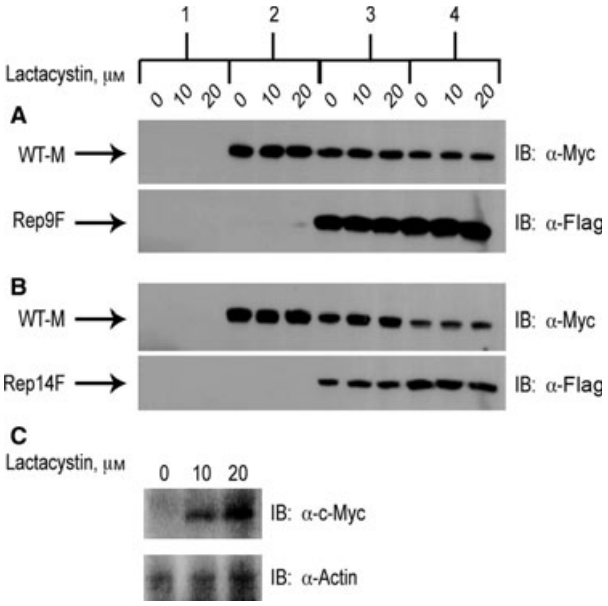

Fig. 7. Lack of effect of lactacystin on degradation of wild-type M6P/IGF2R in response to co-expression with truncated constructs. HEK 293 cells were transfected with the cDNA constructs as indicated: (1) 25 μg pCMV5 vector control; (2) 5 μg WT-M cDNA; (3) 5 μg WT-M + 5 μg mini-receptor cDNAs; (4) 5 μg WT-M + 15 μg mini-receptor cDNAs. Vector control DNA was also added to samples 2 and 3 such that the total amount of DNA transfected per dish was 25 μg. Twenty-four hours after transfection, the cells were treated with the indicated concentrations of lactacystin for 16 h to inhibit proteasomal activity. Detergent extracts were prepared, and 100 μg of total protein from each lysate condition was resolved by 6% SDS/PAGE, immunoblotted with α-FLAG or α-Myc IgGs, and assayed by autoradiography. Arrows indicate the various forms of the M6P/IGF2R expressed in HEK 293 cells. Blots shown are representative of three transfections: co-transfection of WT-M and Rep9F (A) or WT-M and Rep14F (B). (C) Positive control showing the effect of lactacystin on expression of c-Myc (α-Myc IgG at 1 : 500 dilution). Within each transfection group, there was no significant effect of lactacystin on the intensities of the WT-M bands: $P > 0.05$ for all comparisons (A,B).

Rep9F and/or Rep14F individually or in combination were treated with 0, 10 or 20 μM lactacystin for 16 h (Fig. 7). After treatment with lactacystin, cell extracts were analyzed by immunoblotting for expression of each M6P/IGF2R construct (Fig. 7). The amounts of each form of receptor present were not altered by proteasomal inhibition, indicating that the wild-type receptor is not being degraded by this mechanism when truncated receptors are present (Fig. 7A,B, compare the amount of WT-M protein expressed in the presence of 0–20 μM lactacystin for conditions 3 and 4). As a positive control to establish that lactacystin did inhibit proteasomal degradation under these conditions, the levels of c-Myc were assessed. As expected, treatment with lactacystin increased the levels of c-Myc in HEK 293 cell lysates (Fig. 7C).

Release of cell-surface M6P/IGF2Rs into the extracellular medium upon expression of truncated receptors

Proteolytic shedding of the ectodomain of membrane-bound receptors is an evolutionarily conserved post-translational modification by which transmembrane proteins are converted into soluble forms. A soluble

C-terminally truncated form of the M6P/IGF2R has been reported in the serum of several mammalian species [25–28]. This form of the receptor is ~ 20–30 kDa smaller than the intact membrane receptor, and has been shown to lack the cytoplasmic and transmembrane domains [27]. Clairmont *et al*. [28] found that release of the soluble form of the M6P/IGF2R from cells can be blocked by addition of serine protease inhibitors, indicating a proteolytic cleavage event, most likely at the cell surface, followed by release into the medium. To test the possibility that this or a similar mechanism may underlie the dimer interference effects of the Rep9F and Rep14F truncated receptors on the WT-M receptor, we analyzed the expression of M6P/IGF2Rs in cell lysates versus concentrated conditioned medium (CCM) after transfection with truncated receptors (Fig. 8).

The data in Fig. 8 show that the amount of full-length endogenous receptor detected in lysates decreased somewhat as a function of increasing expression of Rep9F (Fig. 8A, upper band), but that expression of Rep14F had little detectable effect on the amount of endogenous M6P/IGF2R in these blots (Fig. 8B). These data contrast with the dramatic effect of truncated receptor expression on the exogenous full-length receptor (WT-M) (compare with data in Fig. 2). This difference may be attributed to level of expression of the truncated receptors in the experiments shown in Fig. 8, which is in better proportion to the amount of endogenous receptor in these cells (note that the bands in Fig. 8A,B were detected by the same antibody, α-M6P/IGF2R, rather than by an antibody against the epitope tag). Nevertheless, we detected large changes in the amounts of a form of endogenous receptor released into the medium in response to expression of both truncated receptors (Fig. 8C,D).

In negative controls expressing no Rep9F or Rep14F, the amount of endogenous M6P/IGF2R found in the CCM is fairly low (Fig. 8C,D; lane 0 μg). As the amount of Rep9F or Rep14F cDNA expressed in the cells increased, several changes were noted in the patterns of endogenous M6P/IGF2R species released. As a function of increasing expression of the Rep9F truncated receptor, we detected increased amounts of the endogenous M6P/IGF2R ectodomain in the CCM samples at the position on the blots corresponding to its calculated molecular mass of 250 kDa (Fig. 8C; lanes 2.5–20 μg). However, a novel high-molecular-mass M6P/IGF2R species (HMM-M6P/IGF2R, indicated by the asterisk in Fig. 8C) also was detected in amounts that corresponded even more closely with the amount of transfected Rep9F. The HMM-M6P/IGF2R may reflect more dramatically the consequences of heterodimeric interactions between the endogenous receptor and this truncated species, leading to increased proteolytic cleavage of the full-length M6P/IGF2R and enhanced release into the extracellular medium. Similarly, expression of the Rep14F truncated receptor enhanced release of both the 250 kDa M6P/IGF2R ectodomain (Fig. 8D) and a novel

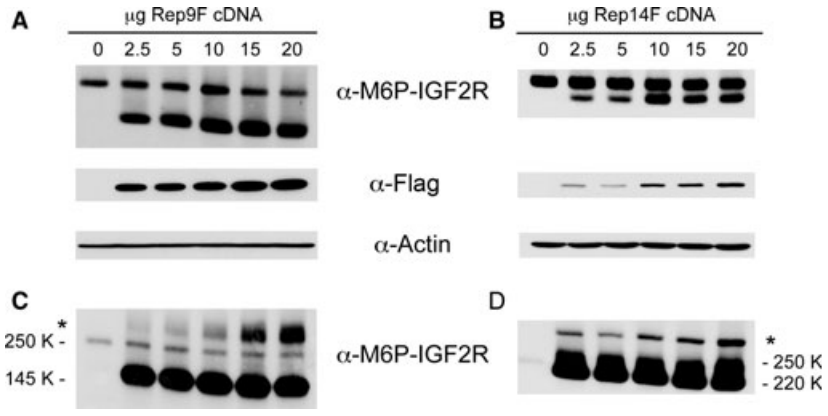

Fig. 8. Proteolytic cleavage of cell-surface M6P/IGF2R is increased in the presence of truncated receptors. Detergent extracts (A,B, 100 μg protein) or concentrated conditioned medium (CCM, C,D, 50 μL volume) from HEK 293 cells transfected with the indicated amounts of the Rep9F or Rep14F cDNA constructs were resolved by 6% SDS/PAGE, immunoblotted with the indicated antibodies, and assayed by autoradiography. Blots representative of at least three transfections are shown: (A,C) Rep9F and (B,D) Rep14F. The asterisks in (C) and (D) indicate the presence of a high-molecular-mass complex of containing M6P/IGF2R but of unknown composition. Regression analysis indicated that the effects of the Rep9F truncated receptor on expression of the full-length receptor in lysates (A, left, $P < 0.03$) and the amount of M6P/IGF2R ectodomain shed into CCM (B, left, $P < 0.0002$) were significant. The effect of the Rep14F truncated receptor on expression of the full-length receptor in lysates (A, right) was significant ($P < 0.02$), but the band intensities for the ectodomain in CCM (B, right) could not be quantified due to lack of resolution from the Rep14F band.

HMM-M6P/IGF2R (Fig. 8D, asterisk). Determining the specific molecular mass of the HMM-M6P/IGF2R species was difficult because these gels were run under non-reducing conditions as required by the antibody. Comparison of the HMM-M6P/IGF2R species present in the Rep9F versus Rep14F transfections indicates that these HMM species are of different mass, consistent with the presence of the truncated Rep9F or Rep14F species in a putative complex. Based on molecular mass values of 145 kDa for the Rep9F protein, 220 kDa for Rep14F and 250 kDa for the cleaved M6P/IGF2R ectodomain, the migration behaviors of the HMM species are consistent with a heterodimeric complex of Rep9F or Rep14F paired with the ectodomain of the endogenous M6P/IGF2R (Fig. 8C versus 8D; note the spacing difference between endogenous (250 K) and HMM (asterisk) M6P/IGF2Rs in the Rep9F versus Rep14F blots).

In contrast to a previous report [28], release of the M6P/IGF2R ectodomain into the medium was not inhibited by any of several serine protease inhibitors tested: phenylmethanesulfonyl fluoride (1 mM), aprotinin (50 mg/ml) or chymostatin (75 μM) (data not shown). Thus, we were unable to replicate the literature findings, and began testing other agents known to block ectodomain release of various cell-surface receptors and cytokines through inhibition of matrix metalloproteinases (MMPs) or members of a disintegrin and metalloproteinase (ADAM) family [29,30]. These enzymes require divalent cations for activity, specifically Zn^{2+}. We therefore used several chelators as an initial broad-based means of testing this possibility. Direct incubation of cells for 48 h with the chelating agents EGTA and EDTA produced some inhibition of ectodomain release (data not shown), but use of 1,10-phenanthroline (OPA), a chelator with strong, but not exclusive, affinity for Zn^{2+}, resulted in striking inhibition of M6P/IGF2R ectodomain release (Fig. 9). OPA at 1–5 mM concentrations produced a pronounced increase in the cellular levels of endogenous full-length receptor (Fig. 9A) and exogenous full-length receptor (WT-M, Fig. 9B), as well as both Rep9F and Rep14F truncated species (Fig 9C,D). Release of all these forms of the receptor was inhibited under these conditions, suggesting that a precursor–product relationship exists in which the presence of soluble receptor in the medium arises from cleavage/release of the cellular M6P/IGF2R. Moreover, the protective effect of OPA on the Rep9F and Rep14F truncated forms suggests that at least some of them remain cell-associated through tethering by dimerization with full-length receptors. Overall, these data are consistent with the hypothesis that ectodomain release

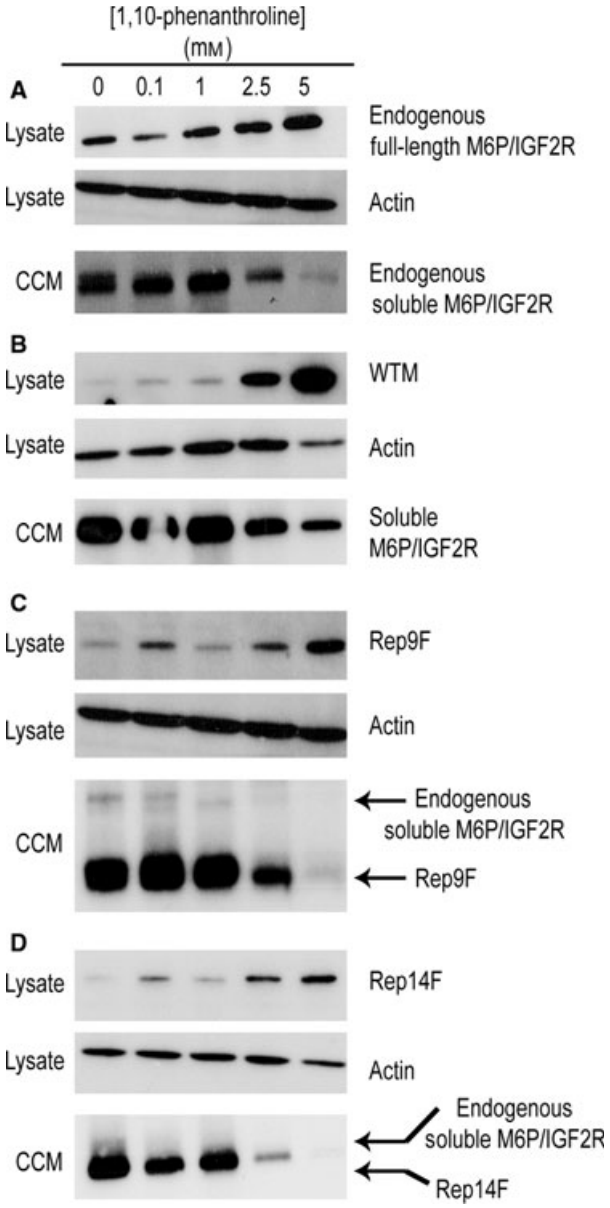

Fig. 9. Inhibition of M6P/IGF2R ectodomain shedding by 1,10-phenanthroline. HEK 293 cells were transfected with empty pCMV5 vector (25 μg DNA) (A) or with the cDNA constructs indicated: (B) 25 μg WT-M cDNA; (C) 25 μg Rep9F cDNA; (D) 25 μg Ref14F cDNA. On the day after transfection, the cells were switched to serum-free medium plus the indicated concentrations of 1,10-phenanthroline. On the third day after transfection, concentrated conditioned medium (CCM) and whole-cell lysates were prepared. Aliquots (100 μg protein) of the lysates and CCM (50 μL volume) were analyzed by immunoblotting with the antibodies indicated on the right. The blots for actin as loading control apply to lysate samples only. These data are representative of three replicate experiments. Regression analysis indicated that the effects of OPA treatment on retention of the various receptor species in lysates were significant: (A) $P < 0.005$; (B) $P < 0.02$; (C) $P < 0.006$; (D) $P < 0.005$.

is mediated by a metalloproteinase, possibly one that is Zn^{2+}-dependent.

Discussion

The original objective of this work was to investigate the implications of M6P/IGF2R dimerization on its function in the biology of IGF-II-stimulated cancers. The oligomeric nature of the M6P/IGF2R has been the subject of considerable investigation since Tong *et al.* [31] reported that binding of monovalent phosphomannosyl ligands such as M6P to the bovine receptor was low-affinity while binding of bivalent ligands was high-affinity. Their work also revealed the stoichiometry of binding as two moles of M6P per mole receptor, suggesting a simple model of one bivalent ligand per receptor. Seminal work by York *et al.* [14] revealed that binding of a multivalent M6P-bearing glycoprotein such as β-glucuronidase promotes cross-bridging of two receptor molecules, and internalization of such ligand-cross-bridged receptors occurred at a three- to fourfold faster rate than when bound to a ligand such as IGF-II that did not stabilize the dimeric structure [14]. M6P/IGF2R dimers cross-bridged by β-glucuronidase transported IGF-II into the cell at the accelerated rate [14]. We have shown that M6P/IGF2R dimerization can occur in the absence of bound phosphomannosyl ligands [16,17]. Dimer formation appears to occur all along the ectodomains of neighboring monomers, with repeat 12 having a special stabilizing role [5,13]. Thus, the current view is that the M6P/IGF2R exists as a dimer in the membrane, and that binding of a bivalent phosphomannosyl ligand cross-bridges M6P binding sites on each monomer, stabilizing the dimeric structure and promoting a conformational change that facilitates endocytosis [32,33].

Many cancers exhibit elevated levels of IGF-II expression that contribute to the growth factor-independent phenotype of the tumors [34]. Mitogenesis driven by IGF-II binding to the insulin-like growth factor I receptor or insulin receptor isoform A supports the rapid-proliferative phenotype of many types of cancer [1,34]. In addition, the M6P/IGF2R may regulate proliferation and migration through its ability to bind and promote activation of plasminogen and transforming growth factor β, as well as to maintain proper sorting of lysosomal enzymes [1,3,9]. Evidence for M6P/IGF2R as a tumor suppressor was obtained initially for hepatocellular carcinoma [15,35,36] and has been the subject of recent reviews [1,12]. Evidence from transgenic animals supports the hypothesis that the growth-suppressive effects of the M6P/IGF2R at the level of the whole animal derive mainly from the receptor's ability to bind pericellular IGF-II and to dispose of it by internalization and subsequent degradation [37,38]. Over-expression of *M6P/IGF2R* inhibited tumorigenesis in a xenograft model using 66c14 mouse mammary tumor cells [8], and when mice slightly over-expressing *M6P/IGF2R* (~ 10% increase over control) were crossed with *Igf2* transgenic mice, tumor formation in the mammary glands of the offspring was significantly delayed [39]. *M6P/IGF2R* mutations of many types have been observed in hepatocellular carcinoma and colon carcinoma, including missense, frameshift and splicing mutations that result in synthesis of truncated proteins [15,18,20,35]. We have investigated the effects of several of these missense mutant forms of the receptor [40,41].

The dimeric structure of the M6P/IGF2R has implications for regulation of IGF-II-driven proliferation and survival in both normal and cancerous cells. There is now evidence that bivalent phosphomannosyl ligands can regulate cell proliferation by modulating the availability of pericellular IGF-II. The protein cellular repressor of E1A-stimulated genes (CREG) is a phosphomannosylated lysosomal glycoprotein that is secreted by some cells [42]. Experiments in several cell lines indicate that secreted CREG can bind to the M6P/IGF2R and inhibit cell proliferation and migration by promoting receptor-mediated uptake and degradation of IGF-II [43–45]. However, there is still some uncertainty in this field, as a recent report indicated that CREG can bind to repeats 11–13 of the M6P/IGF2R in a manner that is independent of CREG glycosylation [46]. Our understanding of this phenomenon is too rudimentary to conclude that M6P-based ligands have a significant physiological role in regulating IGF-II availability in the homeostasis of normal tissues, but the possibility exists that abnormalities in the uptake and lysosomal degradation of IGF-II stimulated by multivalent phosphomannosyl ligands may contribute to the etiology of IGF-II-driven cancers.

Based on this rationale, we hypothesized that mutant M6P/IGF2Rs that interfere with the binding of M6P-based ligands or that create imbalanced receptor heterodimers may also contribute to cancer, either by reducing the level of functional M6P/IGF2R in cells, or, in the context of bi-allelic *M6P/IGF2R* expression when one gene is wild-type and the other mutant, exerting a dominant-negative effect. The mutant M6P/IGF2Rs that seem most likely to produce such effects are truncation mutants of the receptor, of which two are known to occur in cancer. In the present study, we examined the effects of two

cancer-associated mutations that are predicted to produce M6P/IGF2R species truncated in either the 9th or 14th ectodomain repeats [15,18,20]. Our finding that co-expression with a truncated receptor destabilizes the full-length or M6P/IGF2R implies that a tumor cell may enjoy the growth advantages of suppressed M6P/IGF2R activity despite continued expression of wild-type receptor from one good allele, i.e. without loss of heterozygosity.

As a result of the novel observations of apparent instability of the full-length M6P/IGF2R when co-expressed with the cancer-associated truncated forms of receptor, we revised our working hypothesis as to how these mutant receptors influence M6P/IGF2R actions in cells. Our focus shifted to examine the nature of the heterodimer interaction and to uncover the mechanism underlying this instability. Thus, in order to enable tracking of both the truncated and full-length receptor species, we engineered cDNA constructs encoding FLAG-tagged versions of the truncated Rep9 and Rep14 species and studied their effects in co-transfection experiments in HEK 293 cells with full-length Myc-tagged M6P/IGF2R (WT-M). Our data clearly indicate that co-transfection of Rep9F or Rep14F with WT-M at increasing expression ratios suppressed expression of the WT-M receptor. The effect was more dramatic with Rep14F than with Rep9F, which may reflect the possibility that Rep14F was better able to form heterodimers with the full-length receptor. This may be due to the presence of repeat 12 in the Rep14F truncated receptor, which may promote higher-affinity dimerization with WT-M. Rep9F lacks this repeat, which has a prominent role in mediating inter-subunit interactions of the dimeric M6P/IGF2R [5,13]. Support for the hypothesis that this effect arose from formation of heterodimers between the truncated and full-length receptor species in cells was provided by co-immunoprecipitation experiments using detergent lysates of cells. It should be noted that these experiments have not directly shown that heterodimers can form within the membranes of intact cells. In addition, it was always much more difficult to demonstrate co-immunoprecipitation of Rep14F with WT-M, which we attribute to the high degree of instability in this heterodimeric species.

Importantly, transfection of either Rep9F or Rep14F on its own induced instability of the endogenous M6P/IGF2R, suggesting that this phenomenon is not simply an artifact of co-transfection. Again, Rep14F was more potent in this regard than Rep9F. The data obtained by York *et al.* [14] indicating that binding of multivalent phosphomannosyl ligands stabilizes the dimeric structure of the M6P/IGF2R raise another interesting question about the mechanism by which truncated receptors destabilize the wild-type receptor. Ironically, binding of endogenous phosphomannosyl ligands may contribute to degradation of the wild-type receptor by stabilizing heterodimers formed with truncated forms of the receptor. We plan to test this mechanistic possibility in future experiments through use of truncated receptors bearing mutations that knock out the main M6P binding sites in repeats 3 and 9.

To test the hypothesis that heterodimer instability was due to increased receptor degradation, we tested inhibitors of the major protein degradative pathways of the cell. However, chloroquine, an inhibitor of lysosome-mediated degradation, and lactacystin, an inhibitor of the proteasome pathway, had no effect on the receptor instability induced by the truncated M6P/IGF2R species. Comparisons of receptor degradation rates by metabolic labeling followed by immunoprecipitation also showed no effect. We concluded from these studies that if M6P/IGF2R loss is due to instability, that it does not involve any of the conventional pathways for protein breakdown, and that experimental approaches were needed to examine the products of the instability event rather than the intact receptors that remained.

Proteolytic shedding of the ectodomain of membrane-bound receptors is an evolutionarily conserved post-translational modification by which transmembrane proteins are converted into soluble forms. A soluble, C-terminally truncated form of the M6P/IGF2R lacking the cytoplasmic and transmembrane domains was discovered in the blood, amniotic fluid and cerebrospinal fluid of several mammalian species [25–28]. Clairmont *et al.* [28] showed that release of the soluble form of the M6P/IGF2R from BRL-3A rat liver cells was blocked by addition of the serine protease inhibitors aprotinin, chymostatin and phenylmethanesulfonyl fluoride, indicating that the membrane-bound M6P/IGF2R undergoes proteolytic cleavage by a serine protease followed by release into the extracellular environment. However, in our experiments, these same serine protease inhibitors had no effect on the reduction in full-length cellular M6P/IGF2R or the increased release of the M6P/IGF2R ectodomain resulting from expression of the truncated receptors (data not shown). Furthermore, we found that divalent cation-chelating agents, such as EDTA and OPA, not only blocked release of the M6P/IGF2R ectodomain under basal conditions, but also inhibited the increased release that occurred in the presence of the truncated receptors. Thus, we conclude that proteolytic release of the M6P/IGF2R ectodomain does not arise from cleavage

by serine proteases, but instead from cleavage by one or more metalloproteinases. Furthermore, it appears that the receptor instability due to formation of imbalanced heterodimers between full-length and truncated receptor species increases the rate of release by this mechanism.

The phenomenon of proteolytic release of membrane proteins from the cell surface has been observed for many membrane proteins, including cytokines, growth factors, adhesion molecules and their receptors [29,30]. In many cases, the enzymes implicated in these ectodomain shedding events are MMPs, zinc-containing endopeptidases that are involved in the metabolism of the extracellular matrix [47]. MMPs are differentially sensitive to inhibition by divalent metal ion chelators. Some of the MMPs responsible for much of this sheddase activity are members of a disintegrin and metalloproteinase (ADAM) family of zinc metalloproteinases [48–51]. The ADAMs are a large family of transmembrane and secreted proteins with functions in cell adhesion and proteolytic processing of the ectodomains of diverse cell-surface receptors and signaling molecules [51]. They contain a Zn-binding site that is required for catalytic activity. ADAMs 9, 12, 15 and 17 stimulate proliferation of several cancer cell lines. While the current study was in progress, Leksa *et al.* [52] reported that release of the M6P/IGF2R ectodomain was mediated by ADAM17, and not ADAM10, in human umbilical vein endothelial cells. It is not known whether ADAM17-mediated shedding of the M6P/IGF2R ectodomain is universal to all cells, but we are currently testing whether this enzyme mediates the instability of the imbalanced M6P/IGF2R heterodimers produced by the cancer-associated truncation mutants revealed in the present study. Nevertheless, the involvement of ADAM17 or potentially other metalloproteinases in this process provides further support for their important etiological role in cancer, including IGF-II-dependent cancers.

In summary, this study has revealed for the first time that M6P/IGF2R truncation mutants that occur in cancers have a dominant-negative effect on overall expression of the receptor in cells, due to increased shedding of the receptor ectodomain. Our interpretation is that heterodimers of a full-length receptor partnered with a truncated receptor may be more susceptible to cleavage or release from the cell surface. This may arise either from increased accessibility or steric facilitation of cleavage within the juxtamembrane region of the ectodomain of the full-length receptor, as well as the higher probability of release because loss of tethering to the membrane results from a single cleavage event rather than requiring two such cleavage events. Further work is required to identify the metalloproteinase(s) involved and to establish the relevance of this phenomenon to specific cancers.

Experimental procedures

Materials

Oligonucleotides were synthesized by Integrated DNA Technologies (Coralville, IA). D-mannose 6-phosphate (M6P) disodium salt, anti-FLAG M2 IgG, anti-FLAG M2-agarose affinity gel, protein G–Sepharose, the protease inhibitor cocktail (aprotinin, [4-(2-aminoethyl)]benzenesulfonyl fluroride hydrochloride, bestatin hydrochloride, [*N*-(*trans*-epoxysuccinyl)-L-leucine] 4-guanidinobutylamide, leupeptin and pepstatin A), cycloheximide, lactacystin, chloroquine and the bicinchoninic acid kit for protein determination were purchased from Sigma (St Louis, MO). The α-Myc 9E10 IgG was purchased from Upstate Biotechnology Inc. (Hercules, CA), and the α-cathepsin D IgG was purchased from R&D Systems (Minneapolis, MN). The monoclonal anti-CD222 IgG MEM-238 (referred to as α-M6P/IGF2R) was purchased from Abcam (Cambridge, MA, USA). Rabbit α-mouse IgG secondary antibody and the Amicon Ultra centrifugal filters were purchased from Millipore (Billerica, MA, USA). Carrier-free $Na^{125}I$, ^{125}I-protein A and the EasyTag™ EXPRE$^{35}S^{35}S$ protein labeling mix used for the pulse-chase experiments were purchased from PerkinElmer Life Sciences (Waltham, MA). Recombinant human IGFs were purchased from Bachem (Torrance, CA, USA). Radiolabeled IGF-II and unlabeled and radiolabeled pentamannose phosphate–bovine serum albumin (PMP–BSA) were prepared as described previously [41]. The pCMV5 vector was provided by Dr David W. Russell (University of Texas Southwestern Medical Center, Dallas, TX, USA) [53]. The 8.6 kbp human M6P/IGF2R cDNA was provided by Dr William S. Sly (St Louis University Medical Center, St Louis, MO) [54]. Other reagents and supplies were obtained from sources as indicated.

Preparation of epitope-tagged receptors

To study the effects of co-expressing cancer-associated truncated forms of the M6P/IGF2R with full-length receptor in cells, we designed two truncated mini-receptor constructs that mimic naturally occurring cancer-associated forms of the receptor (Fig. 1A) [15,18]. The Rep9F construct encodes repeats 1–8 of the M6P/IGF2R ectodomain and a portion of repeat 9, ending after residue Thr1318 (Fig. 1B). The Rep14F construct encodes repeats 1–13 and part of repeat 14, ending after Ser2023 (Fig. 1C). Both of these constructs include the signal sequence for proper sorting and localization within the cell [55], and each of the mini-receptors bears a C-terminal eight-residue FLAG epitope tag (DYKDDDDK). To produce the Rep9F construct, a

cDNA fragment encompassing nucleotides 94–4103 of the M6P/IGF2R cDNA was cloned into pCMV5RIX [16] using High-Fidelity PCR Supermix (Invitrogen, Life Technologies, Grand Island, NY, USA), a 5′ primer targeted to nucleotides 94–113 followed by an *Xho*I site, and a 3′ primer targeted to nucleotides 4094–4103 followed by a FLAG tag, stop codon and *Xba*I site. This construct was digested using *Eco*RI and *Xba*I and ligated into pCMV5RIX, generating the Rep9F construct (Fig. 1A). For the Rep14F construct, a cDNA fragment encompassing nucleotides 94–6216 of the M6P/IGF2R cDNA, lacking nucleotides 162–5319 that had been previously removed by *Eag*I digestion, was cloned into pCMV5 using a 5′ primer targeted to nucleotides 94–113 followed by a *Kpn*I site, and a 3′ primer targeted to nucleotides 6201–6216 followed by a FLAG tag, two stop codons and an *Xba*I site. This construct was digested using *Kpn*I and *Xba*I and ligated into the pCMV5 vector. The *Eag*I fragment was then inserted into this intermediate construct, producing Rep14F (Fig. 1A). These constructs were designed to mimic the naturally occurring truncations as closely as possible, with a FLAG epitope tag added for ease of purification and detection (Fig. 1B,C). Additionally, 1–15F and WT-M were used as controls in these experiments. The 1–15F construct encodes all 15 repeats of the M6P/IGF2R ectodomain followed by a FLAG epitope tag, cloned into the pCMV5 vector as previously described (Fig. 1A) [16]. The WT-M construct encodes the full-length, wild-type receptor followed by a Myc epitope tag (MEQKLISEEDLN), sub-cloned into the target vector pCMV5 in a multi-stage cloning procedure as previously described [13].

Transient expression of receptor constructs

Human embryonic kidney (HEK 293) cells were maintained in Dulbecco's modified Eagle medium supplemented with 7% fetal bovine serum (Invitrogen/Life Technologies, Grand Island, NY, USA) and grown at 37 °C in a humidified atmosphere of 5% CO_2, 95% air. Transient expression of the various receptor constructs by calcium phosphate-mediated transfection into HEK 293 cells and immunoblot analysis of cell lysates to measure expression of the truncated and full-length receptors were performed as previously described [17,56], except that the chloroquine shock was not performed. Whole-cell lysates were prepared from the 100 mm dishes on the 3rd day after transfection using lysis extraction buffer (50 mM 4-(2-hydroxyethyl)piperazine-1-ethanesulfonic acid, pH 7.4, 1% Triton X-100 and 1 mM $MgCl_2$), as described previously [55]. Following incubation at 4 °C, the suspension was centrifuged at 13 000 ***g*** for 7 min, and the supernatant was collected and stored at −80 °C. Plasma membranes were prepared by Dounce homogenization and differential centrifugation as previously described [57]. Protein concentrations of lysates and plasma membrane suspensions were determined by the bicinchoninic acid assay. For transfections in which conditioned medium was collected, the transfection medium was replaced 24 h post-transfection with serum-free Dulbecco's modified Eagle medium, and incubated on the cells for 48 h. The conditioned medium was collected, supplemented with 1 mM phenylmethanesulfonyl fluoride and 1 mM sodium fluoride, and concentrated using an Amicon Ultra® 10 000 molecular weight cut-off centrifugal filter by centrifuging the samples at 1200 ***g*** for 15 min or until they were concentrated to ∼ 1/20th volume. The protein concentration of the retentate was determined by the bicinchoninic acid assay, and the concentrated conditioned medium (CCM) was stored at −20 °C.

Analysis and expression of M6P/IGF2R constructs

Aliquots (20 μL or 100 μg of total protein as indicated) of Triton X-100 extracts or CCM were resolved by reducing SDS/PAGE and transferred to BA85 nitrocellulose paper (Schleicher & Schuell, Keene, NH, USA). The blots were incubated with blocking buffer (4% non-fat dry milk in 50 mM Hepes, pH 7.6, 150 mM NaCl, 0.1% Tween-20, 0.02% sodium azide) for 1 h at 22 °C, and probed with the appropriate antibody [α-M6P/IGF2R IgG (1 : 4000 dilution), α-FLAG IgG (1 : 1000 dilution) or α-Myc IgG (1 : 500 dilution) in blocking buffer] for 1 h at 22 °C. For the FLAG and Myc blots, a secondary antibody (rabbit α-mouse IgG, 1 : 1000 in blocking buffer) was then used for 30 min at 22 °C. The blots were probed with ^{125}I-protein A (7 μCi in blocking buffer) for 30 min at 22 °C, detected by autoradiography, and quantified using PhosphorImager analysis (Amersham Biosciences Corp., Piscataway, NJ). Ligand blotting analysis with ^{125}I-IGF-II or ^{125}I-PMP–BSA was performed as described previously [58,59].

Dimer formation assays

α-FLAG immunoprecipitation

Aliquots (100 μg) of whole-cell lysates prepared from HEK 293 cells co-transfected with the various cDNAs for the FLAG-tagged mini-receptors and the Myc-tagged M6P/IGF2R were incubated with 8 μL of packed M2 resin in HEPES-buffered saline (HBS) plus 1.0% BSA at 4 °C for 3 h. The resin pellets were collected by centrifugation at 13 000 ***g*** for 30 s, and washed twice for 1 min with 1 ml HBS plus 0.05% Triton X-100 (HBST). Immunoblot analysis was performed by subjecting the resin pellets to treatment with sample buffer plus dithiothreitol, electrophoresis on 6% reducing SDS/PAGE gels, and transfer to BA85 nitrocellulose paper. The blots were probed with either α-FLAG or α-Myc incubated with secondary antibody, followed by ^{125}I-protein A, and detected by autoradiography. Levels of FLAG- and Myc-tagged proteins immunoprecipitated with the M2 resin were quantified by PhosphorImager

analysis of the immunoblots. A second set of gels was run for each condition above containing an equal volume of lysate as a loading control.

α-Myc immunoprecipitation

Aliquots of whole-cell lysates were incubated with 1 μL α-Myc in HBST at 4 °C for 16 h in a total reaction volume of 100 μL. Aliquots (25 μL) of washed protein G–Sepharose resin slurry were added to the overnight incubations together with 75 μL HBS plus 1.0% BSA + 5 mM M6P, and then incubated at 4 °C for 5 h. The resin pellets were collected by centrifugation for 1 min at 6000 ***g*** at 4 °C and washed three times for 1 min at 4 °C with 1 ml HBST. Immunoblot analysis and quantification were performed as described above for the α-FLAG immunoprecipitation assays. A second set of gels was run as a loading control.

Pulse-chase experiments

HEK 293 cells were seeded at 6×10^6 cells per 150 mm dish, and the next day cells were singly or co-transfected with WT-M, Rep9F or Rep14F M6P/IGF2R constructs using calcium phosphate transfection. Prior to labeling, cells were grown to 90% confluence. Medium was then aspirated and replaced by serum-free Dulbecco's modified Eagle's medium lacking L-cystine and L-methionine (Invitrogen). To this was added 0.25 μCi·mL^{-1} ^{35}S-cysteine and ^{35}S-methionine using the EasyTag™ EXPRE^{35}S^{35}S protein labeling mix, 10 μM unlabeled L-methionine and 0.4 mM L-glutamine (pulse medium). Cells were incubated for 30 min at 37 °C, the pulse medium was removed, and the cell monolayers were quickly washed for 1 min with 37 °C serum-free Dulbecco's modified Eagle medium containing 5 mM L-methionine (chase medium). After aspirating the wash medium, 10 ml chase medium was added to the cells and incubated at 37 °C for 0–6 h. At the indicated time points, the chase medium was removed and the cell monolayers were washed with NaCl/P_i at 4 °C. Whole-cell lysates were then subjected to α-Myc or α-FLAG immunoprecipitation and SDS/PAGE. The gels were stained with Coomassie brilliant blue, destained, dried, subjected to autoradiography and quantified by PhosphorImager analysis using a Typhoon model 9410 (GE Healthcare Lifescience, Piscataway, NJ, USA).

Statistical methods

Datasets for which the effect of increasing truncated receptor expression or inhibitor treatments on the amount of full-length receptor was assessed (i.e. Figs 2, 8 and 9) were analyzed by regression analysis. Deviation of the slopes from zero was measured to test the null hypothesis. For experiments involving comparisons of band intensities [absence (control) versus truncated receptor expression or the presence/absence of drug treatment, i.e. Figs 3–5], differences were calculated using a one-way analysis of variance (ANOVA) with Dunnett's test as a post hoc analysis that compared specific group means (e.g. Rep9F and Rep14F) to a control group mean (pCMV5 vector control). Differences were considered significant at $P < 0.05$.

Acknowledgements

We are grateful to Scott Moon, Rachel Riebe, Aaron Pilley, Jennifer Bognich and Philip Van DeVelde for their input and technical support. We thank Dr William S. Sly (St. Louis University Medical Center, St. Louis, MO, USA) for providing the human M6P/IGF2R cDNA and Dr David W. Russell (University of Texas, Southwestern Medical Center, Dallas, TX, USA) for providing pCMV5. We appreciate helpful discussion and suggestions from Dr Richard Lomneth (University of Nebraska at Omaha). This work was supported by National Institutes of Health grant number CA91885 and a grant from the Nebraska Department of Health and Human Services (to R.G.M.), the Nebraska EPSCoR Small Grant Program for Members of Underrepresented Groups in Science in Nebraska (to J.L.K.), and the University Committee on Research and Creative Activity and the College of Arts and Sciences at the University of Nebraska at Omaha (to J.L.K.). M.A.M. was the recipient of pre-doctoral stipend support provided by Graduate Studies and Skala Fellowships through the University of Nebraska Medical Center and a fellowship from the Graduate Assistance in Area of National Need (GAANN) Program from the US Department of Education. This project was also supported by grants from the National Center for Research Resources (5P20RR018759-10) and the National Institute of General Medical Sciences (8 P20 GM103489-10) from the National Institutes of Health.

References

1 Martin-Kleiner I & Gall Troselj K (2010) Mannose-6-phosphate/insulin-like growth factor 2 receptor (M6P/IGF2R) in carcinogenesis. *Cancer Lett* **289**, 11–22.
2 Dahms NM & Hancock MK (2002) P-type lectins. *Biochim Biophys Acta* **1572**, 317–340.
3 Dahms NM (1996) Insulin-like growth factor II/cation-independent mannose 6-phosphate receptor and lysosomal enzyme recognition. *Biochem Soc Trans* **24**, 136–141.
4 El-Shewy HM & Luttrell LM (2009) Insulin-like growth factor-2/mannose-6-phosphate receptors. *Vitam Horm* **80**, 667–697.

5 Brown J, Delaine C, Zaccheo OJ, Siebold C, Gilbert RJ, van Boxel G, Denley A, Wallace JC, Hassan AB, Forbes BE *et al*. (2008) Structure and functional analysis of the IGF-II/IGF2R interaction. *EMBO J* **27**, 265–276.
6 O'Gorman DB, Costello M, Weiss J, Firth SM & Scott CD (1999) Decreased insulin-like growth factor-II/mannose 6-phosphate receptor expression enhances tumorigenicity in JEG-3 cells. *Cancer Res* **59**, 5692–5694.
7 O'Gorman DB, Weiss J, Hettiaratchi A, Firth SM & Scott CD (2002) Insulin-like growth factor-II/mannose 6-phosphate receptor overexpression reduces growth of choriocarcinoma cells *in vitro* and *in vivo*. *Endocrinology* **143**, 4287–4294.
8 Li J & Sahagian GG (2004) Demonstration of tumor suppression by mannose 6-phosphate/insulin-like growth factor 2 receptor. *Oncogene* **23**, 9359–9368.
9 Leksa V, Godár S, Cebecauer M, Hilgert I, Breuss J, Weidle UH, Horejsí V, Binder BR & Stockinger H (2002) The N terminus of mannose 6-phosphate/insulin-like growth factor 2 receptor in regulation of fibrinolysis and cell migration. *J Biol Chem* **277**, 40575–40582.
10 Olson LJ, Dahms NM & Kim J-JP (2004) The N-terminal carbohydrate recognition site of the cation-independent mannose 6-phosphate receptor. *J Biol Chem* **279**, 34000–34009.
11 Olson LJ, Yammani RD, Dahms NM & Kim J-JP (2004) Structure of uPAR, plasminogen, and sugar-binding sites of the 300 kDa mannose 6-phosphate receptor. *EMBO J* **223**, 2019–2028.
12 Brown J, Jones EY & Forbes BE (2009) Keeping IGF-II under control: lessons from the IGF-II–IGF2R crystal structure. *Trends Biochem Sci* **34**, 612–619.
13 Kreiling JL, Byrd JC & MacDonald RG (2005) Domain interactions of the insulin-like growth factor II/mannose 6-phosphate receptor. *J Biol Chem* **280**, 21067–21077.
14 York SJ, Arneson LS, Gregory WT, Dahms NM & Kornfeld S (1999) The rate of internalization of the mannose 6-phosphate/insulin-like growth factor II receptor is enhanced by multivalent ligand binding. *J Biol Chem* **274**, 1164–1171.
15 De Souza AT, Hankins GR, Washington MK, Orton TC & Jirtle RL (1995) *M6P/IGF2R* gene is mutated in human hepatocellular carcinomas with loss of heterozygosity. *Nat Genet* **11**, 447–449.
16 Byrd JC & MacDonald RG (2000) Mechanisms for high affinity mannose 6-phosphate ligand binding to the insulin-like growth factor II/mannose 6-phosphate receptor. Negative cooperativity and receptor oligomerization. *J Biol Chem* **275**, 18638–18646.
17 Byrd JC, Park JHY, Schaffer BS, Garmroudi F & MacDonald RG (2000) Dimerization of the insulin-like growth factor II/mannose 6-phosphate receptor. *J Biol Chem* **275**, 18647–18656.
18 Souza RF, Appel R, Yin J, Wang S, Smolinski KN, Abraham JM, Zou T-T, Shi Y-Q, Lei J, Cottrell J *et al*. (1996) Microsatellite instability in the insulin-like growth factor II receptor gene in gastrointestinal tumours. *Nat Genet* **14**, 255–257.
19 Ouyang H, Shiwaku HO, Hagiwara H, Miura K, Abe T, Kato Y, Ohtani H, Shiiba K, Souza RF, Meltzer SJ *et al*. (1997) The insulin-like growth factor II receptor gene is mutated in genetically unstable cancers of the endometrium, stomach, and colorectum. *Cancer Res* **57**, 1851–1854.
20 Kong F-M, Anscher MS, Washington MK, Killian KJ & Jirtle RL (2000) *M6P/IGF2R* is mutated in squamous cell carcinoma of the lung. *Oncogene* **19**, 1572–1578.
21 Sahagian GG (1984) The mannose 6-phosphate receptor: function, biosynthesis and translocation. *Biol Cell* **51**, 207–214.
22 MacDonald RG & Czech MP (1985) Biosynthesis and processing of the type II insulin-like growth factor receptor in H-35 hepatoma cells. *J Biol Chem* **260**, 11357–11365.
23 Blok J, Mulder-Stapel AA, Ginsel LA & Daems WT (1981) The effect of chloroquine on lysosomal function and cell-coat glycoprotein transport in the absorptive cells of cultured human small-intestinal tissue. *Cell Tissue Res* **218**, 227–251.
24 Jockers R, Angers S, Da Silva S, Benaroch P, Strosberg AD, Bouvier M & Marullo S (1999) β_2-adrenergic receptor down-regulation. Evidence for a pathway that does not require endocytosis. *J Biol Chem* **274**, 28900–28908.
25 Kiess W, Greenstein LA, White RM, Lee L, Rechler MM & Nissley SP (1987) Type II insulin-like growth factor receptor is present in rat serum. *Proc Natl Acad Sci USA* **84**, 7720–7724.
26 Causin C, Waheed A, Braulke T, Junghans U, Maly P, Humbel RE & von Figura K (1988) Mannose 6-phosphate/insulin-like growth factor II-binding proteins in human serum and urine. Their relation to the mannose 6-phosphate/insulin-like growth factor II receptor. *Biochem J* **252**, 795–799.
27 MacDonald RG, Tepper MA, Clairmont KB, Perregaux SB & Czech MP (1989) Serum form of the rat insulin-like growth factor II/mannose 6-phosphate receptor is truncated in the carboxyl-terminal domain. *J Biol Chem* **264**, 3256–3261.
28 Clairmont KB & Czech MP (1991) Extracellular release as the major degradative pathway of the insulin-like growth factor II/mannose 6-phosphate receptor. *J Biol Chem* **266**, 12131–12134.
29 Black RA (2002) Tumor necrosis factor-alpha converting enzyme. *Int J Biochem Cell Biol* **34**, 1–5.
30 Mullberg J, Althoff K, Jostock T & Rose-John S (2000) The importance of shedding of membrane proteins for cytokine biology. *Eur Cytokine Netw* **11**, 27–38.

31 Tong PY, Gregory W & Kornfeld S (1989) Ligand interactions of the cation-independent mannose 6-phosphate receptor. The stoichiometry of mannose 6-phosphate binding. *J Biol Chem* **264**, 7962–7969.
32 Ghosh P, Dahms NM & Kornfeld S (2003) Mannose 6-phosphate receptors: new twists in the tale. *Nat Rev Mol Cell Biol* **4**, 202–213.
33 MacDonald RG & Byrd JC (2003) The insulin-like growth factor II/mannose 6-phosphate receptor: implications for IGF action in breast cancer. *Breast Dis* **17**, 61–72.
34 Pollak MN, Schernhammer ES & Hankinson SE (2004) Insulin-like growth factors and neoplasia. *Nat Rev Cancer* **4**, 505–518.
35 De Souza AT, Hankins GR, Washington MK, Fine RL, Orton TC & Jirtle RL (1995) Frequent loss of heterozygosity on 6q at the mannose 6-phosphate/insulin-like growth factor II receptor locus in human hepatocellular tumors. *Oncogene* **10**, 1725–1729.
36 Hankins GR, De Souza AT, Bentley RC, Patel MR, Marks JR, Iglehart JD & Jirtle RL (1996) M6P/IGF2 receptor: a candidate breast tumor suppressor gene. *Oncogene* **12**, 2003–2009.
37 Filson AJ, Louvi A, Efstratiadis A & Robertson EJ (1993) Rescue of the T-associated maternal effect in mice carrying null mutations in *Igf-2* and *Igf2r*, two reciprocally imprinted genes. *Development* **118**, 731–736.
38 Ludwig T, Eggenschwiler J, Fisher P, D'Ercole AJ, Davenport ML & Efstratiadis A (1996) Mouse mutants lacking the type 2 IGF receptor (IGF2R) are rescued from perinatal lethality in *Igf2* and *Igf1r* null backgrounds. *Dev Biol* **177**, 517–535.
39 Wise TL & Pravtcheva DD (2006) Delayed onset of *Igf2*-induced mammary tumors in *Igf2r* transgenic mice. *Cancer Res* **66**, 1327–1336.
40 Devi GR, De Souza AT, Byrd JC, Jirtle RL & MacDonald RG (1999) Altered ligand binding by insulin-like growth factor II/mannose 6-phosphate receptors bearing missense mutations in human cancers. *Cancer Res* **59**, 4314–4319.
41 Byrd JC, Devi GR, De Souza AT, Jirtle RL & MacDonald RG (1999) Disruption of ligand binding to the insulin-like growth factor II/mannose 6-phosphate receptor by cancer-associated missense mutations. *J Biol Chem* **274**, 24408–24416.
42 Schähs P, Weidinger P, Probst OC, Svoboda B, Stadlmann J, Beug H, Waerner T & Mach L (2008) Cellular repressor of E1A-stimulated genes is a bona fide lysosomal protein which undergoes proteolytic maturation during its biosynthesis. *Exp Cell Res* **314**, 3036–3047.
43 Di Bacco A & Gill G (2003) The secreted glycoprotein CREG inhibits cell growth dependent on the mannose-6-phosphate/insulin-like growth factor II receptor. *Oncogene* **22**, 5436–5445.
44 Han Y, Cui J, Tao J, Guo L, Guo P, Sun M, Kang J, Zhang X, Yan C & Li S (2009) CREG inhibits migration of human vascular smooth muscle cells by mediating IGF-II endocytosis. *Exp Cell Res* **315**, 3301–3311.
45 Han Y-L, Guo P, Sun M-Y, Guo L, Luan B, Kang J, Yan C-H & Li S-H (2008) Secreted CREG inhibits cell proliferation mediated by mannose 6-phosphate/insulin-like growth factor II receptor in NIH3T3 fibroblasts. *Genes Cells* **13**, 977–986.
46 Han Y-L, Luan B, Sun M, Guo L, Guo P, Tao J, Deng J, Wu G, Liu S, Yan C *et al.* (2011) Glycosylation-independent binding to extracellular domains 11–13 of mannose-6-phosphate/insulin-like growth factor-2 receptor mediates the effects of soluble CREG on the phenotypic modulation of vascular smooth muscle cells. *J Mol Cell Cardiol* **50**, 723–730.
47 Seals DF & Courtneidge SA (2003) The ADAMs family of metalloproteases: multidomain proteins with multiple functions. *Genes Dev* **17**, 7–30.
48 Arribas J & Massague J (1995) Transforming growth factor-α and β-amyloid precursor protein share a secretory mechanism. *J Cell Biol* **128**, 433–441.
49 Hundhausen C, Misztela D, Berkhout TA, Broadway N, Saftig P, Reiss K, Hartmann D, Fahrenholz F, Postina R, Matthews V *et al.* (2003) The disintegrin-like metalloproteinase ADAM10 is involved in constitutive cleavage of CX3CL1 (fractalkine) and regulates CX3CL1-mediated cell–cell adhesion. *Blood* **102**, 1186–1195.
50 Duffy MJ, McKiernan E, O'Donovan N & McGowan PM (2009) Role of ADAMs in cancer formation and progression. *Clin Cancer Res* **15**, 1140–1144.
51 Edwards DR, Handsley MM & Pennington CJ (2008) The ADAM metalloproteinases. *Mol Aspects Med* **29**, 258–289.
52 Leksa V, Loewe R, Binder B, Schiller HB, Eckerstorfer P, Forster F, Cardona AS, Ondrovicova G, Kutejova E, Steinhuber E *et al.* (2011) Soluble M6P/IGF2R released by TACE controls angiogenesis via blocking plasminogen activation. *Circ Res* **108**, 676–685.
53 Andersson S, Davis DL, Dahlbäck H, Jörnvall H & Russell DW (1989) Cloning, structure, and expression of the mitochondrial cytochrome P-450 sterol 26-hydroxylase, a bile acid biosynthetic enzyme. *J Biol Chem* **264**, 8222–8229.
54 Oshima A, Nolan CM, Kyle JW, Grubb JH & Sly WS (1988) The human cation-independent mannose 6-phosphate receptor. Cloning and sequence of the full-length cDNA and expression of functional receptor in COS cells. *J Biol Chem* **263**, 2553–2562.
55 Garmroudi F, Devi G, Slentz DH, Schaffer BS & MacDonald RG (1996) Truncated forms of the insulin-like growth factor II (IGF-II)/mannose 6-phosphate receptor encompassing the IGF-II binding site:

characterization of a point mutation that abolishes IGF-II binding. *Mol Endocrinol* **10**, 642–651.

56 Pear WS, Nolan GP, Scott ML & Baltimore D (1993) Production of high-titer helper-free retroviruses by transient transfection. *Proc Natl Acad Sci USA* **90**, 8392–8396.

57 Schaffer BS, Lin M-F, Byrd JC, Park JHY & MacDonald RG (2003) Opposing roles for the insulin-like growth factor (IGF)-II and mannose 6-phosphate (Man-6-P) binding activities of the IGF-II/Man-6-P receptor in the growth of prostate cancer cells. *Endocrinology* **144**, 955–966.

58 Hossenlopp P, Seurin D, Segovia-Quinson B, Hardouin S & Binoux M (1986) Analysis of serum insulin-like growth factor binding proteins using Western blotting: use of the method for titration of the binding proteins and competitive binding studies. *Anal Biochem* **154**, 138–143.

59 Hartman MA, Kreiling JL, Byrd JC & MacDonald RG (2009) High-affinity ligand binding by wild-type/mutant heteromeric complexes of the mannose 6-phosphate/insulin-like growth factor II receptor. *FEBS J* **27**, 1915–1919.